RSC Advances

RSC Advances

www.rsc.org/advances

ROYAL SOCIETY
OF CHEMISTRY

www.rsc.org/advances

Please do not adjust margins

RSC Advances

Journal Name

ARTICLE

Microwave synthesis of carbon dots with multi-response using denatured proteins as carbon source

Xue Liu, Tianze Li, Yu Hou, Qiuhua Wu, Jie Yi and Guolin Zhang*

A new synthetic strategy has been developed for facile and green fabrication of highly photoluminescent carbon dots (CDs) via a one-step microwave treatment of the denatured proteins in aqueous solution. The as-prepared CDs, possessing excellent up-conversion fluorescent properties, can serve as a multifunctional fluorescent nanosensor for pH and temperature. CDs prepared from various protein carbon source can be sensitive to a specific metal ion.

1.Introduction

Fluorescent carbon dots (CDs) are one of the rising stars in carbonaceous nanomaterials, which have attracted tremendous attention due to their intriguing optical, chemical and biological properties.[1-2] Compared with traditional fluorescent semiconductor quantum dots (QDs), composed of heavy metals as the essential photoluminescent elements, CDs are advantageous in their green synthesis and biocompatibility. Great efforts have been devoted to apply CDs in biological fields instead of QDs, including bioimaging,[3-6] biosensors,[7-9] and so on. CDs can be prepared in large quantities from various carbon sources,[10-14] including even some waste carbon sources,[14] using a variety of environmentally benign physical and chemical means.[15-16] Therefore, CDs can be considered as the ideal nanomaterials satisfying the Principles of Green Chemistry, which maximize their application performance and minimize undesirable implications.[17]

Along with the deepening research in CDs, the chemical structure and physical properties of CDs are gradually clear.[1-2] In many ways, CDs resemble graphene oxides (GODs), which preserves the layer structure of the parent graphite, equipped with oxygen epoxide groups (bridging oxygen atoms), carbonyl, hydroxyl, and so on.[18] The distinction between CDs and GODs mainly comes from the size difference, where CDs usually refer to the carbonaceous, graphitic nanoparticles with size below 10 nm. The formation mechanism of CDs is also demonstrated in some studies.[19-22] For example, Yu's group used citric acid and monoethanolamine to prepare nitrogen-doped CDs.[22] Transmission electron microscopy (TEM), ultraviolet-visible absorbance spectroscopy (UV-Vis) and

photoluminescence spectroscopy (PL) were applied to monitor the formation process of CDs. A four-step forming mechanism of CDs including polymerization, aromatization, nucleation and growth was proposed. The intermolecular dehydration polymerization among carbon source and stabilizing agents has been assumed as the first stage during the forming process of CDs,[19-22] and therefore some polymers were also directly applied as carbon source or stabilizing agents to prepare CDs.[23-24]

Proteins are natural bio-macromolecules, and under some conditions, proteins can unfold into peptide-polymers.[25] These peptide-polymers, which impart biocompatibility and high stability in an aqueous environment, possess a precisely known length of the main chain and a distinct number of functional groups at defined locations. These multiple functional groups can facilitate further modifications for various applications and serve as effective stabilizing agents in such formulations.[26-33] For example, Chan and co-workers used denatured human serum albumins (dHSAs) to direct the synthesis of graft copolymer dHSA-PEG,[31] which can cover QDs to improve their hydrophilicity and stability. Irudayaraj and co-workers applied denatured bovine serum albumins (dBSAs) to synthetize fluorescent Ag clusters in aqueous solutions.[33] The dBSAs with 35 cysteine residues can act as a polyvalent ligand to stabilize the metal core. Proteins were also used as the natural carbon source to construct CDs. Zheng and co-workers prepared a kind of particular hollow CDs from BSA by solvothermal reaction.[34] Because of the specific hollow nanostructure and photoluminescence properties, the as-prepared CDs show potential for application in both drug delivery and cell imaging. However, the quantum yields of the as-prepared CDs was not ideal, and reached only 7%. Besides, in this research, solvothermal method was not economic, which consumed amounts of energy and time. The relatively low quantum yields can be attributable to the folded structure of BSA, which can't fully and thoroughly participate in the forming process of CDs. Therefore, in this work, we denatured BSA first of all and transformed BSA into linear peptide-

Liaoning Province Key Laboratory for Green Synthesis and Preparative Chemistry of Advanced Materials, College of Chemistry, Liaoning University, Shenyang, 110036, (P. R. China), Fax: (+86) 24-6220-2380, E-mail: glzhang@lnu.edu.cn
Electronic Supplementary Information (ESI) available: [details of any supplementary information available should be included here]. See DOI: 10.1039/x0xx00000x

RSC Advances Accepted Manuscript

polymers, and then CDs were prepared using the peptide-polymers as the carbon source. The peptide-polymers can participate in the preparing process more effectively, which is beneficial for the formation of CDs. Moreover, microwave irradiation method was taken in this system, resulting in time and energy saving processes and suppressing undesired side-reactions, which finally made the as-prepared CDs with a higher quantum yields of 14%. The as-prepared CDs possess up-conversion fluorescent properties, which can act as nanosensor for pH, temperature and metal ions. Most interestingly, CDs prepared from different protein carbon source can be sensitive to a specific metal ion. For example, BSA-CDs (CDs prepared from bovine serum albumins) show a selective detection for Ag^+, while pepsin-CDs and lipase-CDs show a selective detection for Cu^{2+} and Ni^{2+} respectively.

2. Materials and methods

2.1 Chemicals and materials

Bovine serum albumin (BSA), lipase, pepsase, guanidine hydrochloride and quinine sulfate dehydrate (98%) were purchased from Aladdin Industrial Corporation and used without further purification. Urea was purchased from Tianjin Damao Chemical Reagent Factory (Tianjin, China). All the other reagents were purchased from Sinopharm Chemical Reagent Company Limited (Shanghai, China). All the solvents were of analytical grade and used as received. Ultrapure water was used in all experiments.

2.2 Preparation of CDs

CDs were prepared from BSA and urea via a one-step microwave treatment. In a typical procedure, BSA (0.03 g) and urea (2.4 g) were dissolved in ultrapure water (5 mL) to form a transparent homogeneous solution. The solution was stirred and incubated overnight to denature BSA, and then the mixed solution was put into a domestic microwave oven and heated for about 5 minutes (700 W). The solution turned into brown crude CDs solid. After cooling down to room temperature, ultrapure water (15 mL) was added to dissolve the crude CDs, assisted by ultrasonic vibrations. The resultant light yellow solution was separated by centrifugation at 10,000 rpm for 30 minutes. The supernatant was then dialyzed against ultrapure water through a dialysis membrane (molecular weight cut off=8000-14000, Shanghai Baoman Biological technology Co. LTD) for 48 hours to remove the excess precursors and small molecules. The resultant CDs solution were maintained at 4 °C for further characterization and use.

Apart from BSA, the other protein carbon sources, including lipase and pepsase, were also applied to prepare CDs. The mole concentration of these two proteins kept in step with that of the previous BSA (9.0×10^{-5} M). Guanidine hydrochloride, another denaturing agent was also used to denature BSA and then prepare CDs, the concentration of which was identical to urea (8.0 M).

2.3 Calculation of fluorescence quantum yields

The quantum yield of the CDs was determined by a comparative method.[35] Quinine sulfate in 0.1 M H_2SO_4 (literature quantum yield: 54%) was selected as a standard sample to calculate the QY of test sample (i.e. CDs) which was dissolved in ultrapure water at different concentrations. All the absorbance values of the solutions at the excitation wavelength were measured with UV-Vis spectrophotometer. Fluorescence emission spectra of all the sample solutions were recorded by fluorometer at an excitation wavelength of 360 nm. The integrated fluorescence intensity is the area under the fluorescence curve in a different wavelength range. Then a graph was plotted using the integrated fluorescence intensity against the absorbance and a trend line was added for each curve with intercept at zero. Absolute values were calculated according to the following equation:

$$\Phi_x = \Phi_{ST}\left(\frac{Grad_X}{Grad_{ST}}\right)\left(\frac{\eta_X^2}{\eta_{ST}^2}\right)$$

Where the subscripts ST and X denote standard and test respectively, Φ is the fluorescence quantum yield, Grad is the gradient from the plot of integrated fluorescence intensity vs absorbance, and η is the refractive index of the solvent. In order to minimize re-absorption effects, absorbance in the 10 mm fluorescence cuvette should never exceed 0.1 at the excitation wavelength.

2.4 Fluorescence assay of Ag^+

Taking 3.2 mL CD solution with the absorbance of 0.05 (λ_{ab}=360 nm), 0.8 mL Ag^+ PBS buffer with a calculated concentration (0, 0.1, 0.5, 1, 1.5, 2, 3, 4, 5, 6, 8, 10, 12, 15 and 20 μM) was added and the fluorescence spectra were recorded (λ_{ex}=360 nm). There existed a standard curve for the maximal fluorescence intensity to the concentration of Ag^+, and quantitative Ag^+ concentration detection can be conducted according to the standard curve. All the sensitivity and selectivity measurements were conducted in triplicate.

For analysis of real samples, local tap water was freshly collected without any pretreatment. A standard addition method was applied to evaluate the validity of the as-prepared CD sensor. The procedure was similar to the above-mentioned assay of Ag^+, except that the solutions added into the CD solution were 0.4 mL of tap water and 0.4 mL of Ag^+ PBS buffer (0, 1, 3, 5 and 7 μM).

2.5 Instruments and measurements

UV-Vis absorption was measured on a Lambda Bio 20 (Perkin Elmer, America). PL measurements were performed using F-7000 (FL Spectrophotometer, Japan), equipped with a thermostated cell holder. The excitation and emission slit is 5 and 5 nm, respectively. The normalized spectra were obtained by dividing each fluorescence intensity of the fluorescence spectrum by the maximum value of its own. The morphology and microstructure of the CDs were examined by high-resolution transmission electron microscopy (HRTEM) on a

JEM-2100 (JEOL, Japan) with an accelerating voltage of 200 kV. The samples for HRTEM were made by dropping an aqueous solution onto a 200-mesh copper grid coated with a lacy carbon film. The size distribution tests were determined by dynamic light scattering (DLS) using a Malvern Nano ZS instrument. Fourier transform infrared spectroscopy (FTIR) spectra were collected by a Perkin-Elmer FT-IR spectrometer using KBr pellets. X-ray diffraction (XRD, Bruber, Germany) was conducted with Cu-Kα radiation (40 kV, 40 mA, 5° min[-1]) and 2θ range of 20-60[o]. Raman spectrum was gained on a Renishaw inVia 2000 Raman system equipped with a 514 nm laser. The X-ray photoelectron spectra (XPS) were recorded using a K-alpha spectrometer (Thermo Fisher, UK).

3. Results and discussions

3.1 Structure and composition of CDs

The formation of CDs can be confirmed through UV-Vis, FTIR, XRD, Raman and XPS. The UV-Vis spectrum of CDs in Fig.1a shows typical optical absorption in the UV region, with a tail extending to the visible range similar to that of previously reported CDs.[1] There exist two main absorption features in the spectrum: an intensive peak at 236 nm due to the $\pi-\pi^*$ transition of C=C bonds; a shoulder peak at 283 nm assigned to the $n-\pi^*$ transition of C=O bonds.[36] In the FTIR spectrum of CDs in Fig. 1b, the vibration band of C=C at 1615 cm^{-1} confirms the carbonization of proteins under microwave irradiation. In addition, there are more apparent hydrophilic functional groups on the surface of CDs, as shown by the vibration bands of -OH, $-NH_2$ and C-O-C groups at 3000-3750 cm^{-1}.[37] The CDs show XRD patterns of disordered carbon (Fig. 1c), with an (002) interlayer spacing of 4.0 Å, which is larger than that of bulk graphite (3.3 Å), indicating poor crystallization.[2] An apparent G band at 1530 cm^{-1} and a weak D band at 1340 cm^{-1} are observed in the Raman spectrum of CDs (Figure 1d), indicating there are mainly sp[2] carbons with some sp[3] hybrid carbons in the as-prepared CDs.[38] The XPS spectra of CDs (Fig. 1e) exhibit three peaks at 289.0, 400.0 and 532.0 eV, which are attributed to C 1s, N 1s, and O 1s, respectively.[39] The results indicate that the as-prepared CDs contain carbon, nitrogen, and oxygen in a weight ratio of 46.80 : 31.04 : 22.16. In detail, the high-resolution C 1s spectrum (Fig. 1f) shows three peaks at 284.5, 286.3 and 289.4 eV, which are attributed to C-C/C=C, C-O and N-C=O respectively.[40] The high-resolution N 1s and O 1s spectra are shown in the supporting information (Fig. S1 and S2), further showing the chemical composition and structure message of CDs.[41-42]
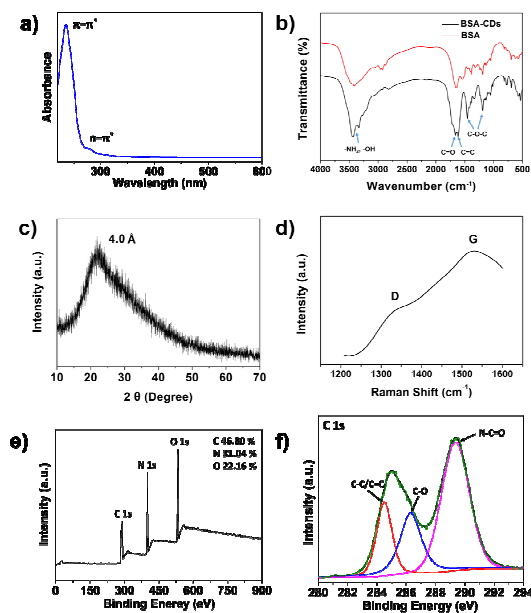
Fig. 1 a) UV-Vis absorption spectrum of CDs (The concentration of CDs is 10.0 mg/mL); b) FTIR spectra of BSA-CDs and BSA; c) XRD pattern of CDs; d) Raman spectrum of CDs; e) Survey XPS data of CDs; f) High-resolution C 1s XPS spectra of CDs.

HRTEM and DLS tests were used to determine the shape, size and nature of the as-prepared CDs (Fig. 2). The CDs are spherical nanoparticles with an average size of 5.4±2.3 nm in Fig. 2a (Particle size distribution analysis was carried out by counting 20 particles from the TEM image.). Regions of both graphitic and amorphous carbon can be seen from the magnified HRTEM image (Fig. 2a inset); the graphitic regions show lattice fringes. The statistical diameter distribution data (Fig. 2b) shows a CD size range from 2.4 to 5 nm, similar to that observed from the HRTEM images.
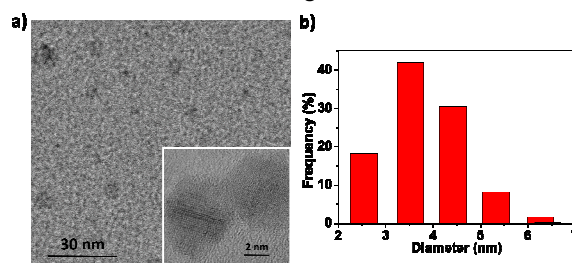
Fig. 2 a) HRTEM images of CDs (inset: magnified HRTEM images); b) size distribution of CDs.

The protein carbon source shows no fluorescence emission, while the as-prepared CDs show a strong fluorescence emission with an emission peak located at ca. 400 nm (Fig. 3, λ_{ex}=360 nm). Using quinine sulfate as the reference, the fluorescence quantum yield (QY) of the CDs was checked as 14%. The fluorescence emission spectra of CDs excited by various excitation wavelengths are shown in Fig. 3a. The

ARTICLE   **Journal Name**

excitation wavelength dependence of the emission wavelength and the normalized fluorescence intensity are listed in Fig. 3b. With increasing excitation wavelengths, the position of the fluorescence emission peaks for CDs gradually red-shifts, while the emission peak intensity increases at first and then decreases after reaching a maximum at 360 nm. The excitation wavelength dependence of the emission wavelength and the normalized fluorescence intensity of the maximum fluorescence emission are shown in Fig. 3b, which reflects not only the size effects of CDs, but also a considerable distribution of emissive trap sites on each CD.[1-2] Besides, the excitation wavelength dependence of PL behavior can be readily observed by naked eye as well (Figure 3 d).

propose a formation mechanism of the CDs prepared from protein carbon source (Scheme 1). First of all, proteins are denatured into unfolded peptide chain (Scheme 1a). Compared with the small molecules carbon source reaction system, which needs a polymerization stage, the protein peptide chains experience an intermolecular dehydration and crosslinking (Scheme 1b). Keeping microwave heating, intramolecular dehydration takes place and a number of C=C and C=N bonds form inside the peptide network, which results in aromatic clusters precursor for CDs (Scheme 1c). When the concentration of aromatic clusters in some local areas of the peptide microgel reaches the critical supersaturation point, a burst in the nucleation of CDs will take place (Scheme 1d).[43]
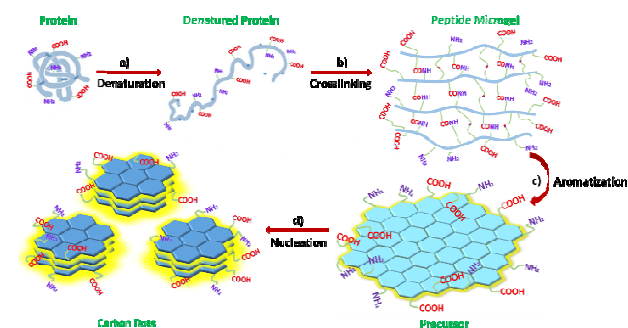
Scheme 1. The formation mechanism of CDs prepared from protein carbon source.

The forming mechanism of CDs can be confirmed from the variation of the grain diameter and fluorescence spectra of CDs with reaction time. As shown in Fig. 4a and b, the fluorescence intensity of CDs increases with the microwave treating time, and meanwhile their grain diameter reaches a maximum when the microwave treating time is 3 minutes. Interestingly, these phenomena correspond to the various stages of the forming process of CDs. Originally, a transparent homogenous solution with a certain amount of water is necessary for carbonization uniformity (Fig. 4a and b, 0 minutes). With microwave heating, the water is evaporated and the dehydration reaction proceeds, which results in the intermolecular crosslinking peptide microgel with a lager grain diameter but without fluorescence emission (Fig. 4a and b, 1 minute). Further microwave heating induces the aromatization process, and the CD precursors come into being (Fig. 4a and b, 3 minutes). Compared with the final CDs, the CD precursors show a weaker fluorescence emission however a larger grain diameter (Fig. 4a and b, 5 minutes). Proteins without urea denaturing were also monitored with microwave treating (Fig. 4c and d). With the increase of heating time, thermal denaturing happens to proteins, and proteins peptide gradually expose more and more hydrophobic groups, which results in the final intermolecular aggregate (Fig. 4c). Hydrophobic aggregation is unfavorable for the aromatization and nucleation of CDs, so no fluorescence emission is observed during incubating BSA solution under microwave irradiation (Fig. 4d). It is noteworthy that, the mechanisms of protein

Fig. 3 a) PL spectra of CDs excited progressively from 300 to 420 nm with 20 nm increments of excitation wavelengths. b) Excitation wavelength dependence of the emission wavelength and the normalized fluorescence intensity of CDs fluorescence emission. c) Photographs of aqueous solution dispersed with CDs under various excitation wavelengths. (The concentration of CDs is 5 mg/mL)

3.2 Formation mechanism of CDs

For the previously reported CDs prepared from small molecular carbon source, there exists a speculation about their forming process, including four stages: polymerization, aromatization, nucleation and growth.[19-22] Based on this, we

denaturation using denaturing agents and hyperthermia are different. Denaturing agents, such as urea and guanidine hydrochloride, can interact with proteins and form intermolecular hydrogen bonds, which screens intramolecular hydrogen bonds of proteins.[44] Meanwhile denaturing agents also diminish the hydrophobic effect and facilitate the exposure of the hydrophobic core residues.[44] However, when exposed to harsh conditions (e.g., high temperature), partially owing to the lack of mechanisms that prevent misfolded/unfolded proteins, they are prone to aggregate and lose their bio-functions.[45]
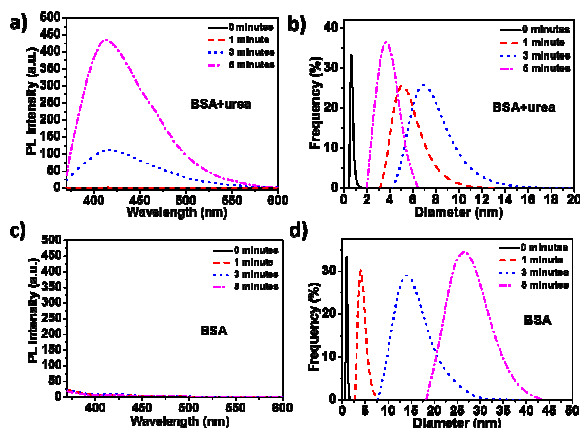
Fig. 4 Size distributions of BSA a) with and b) without urea treatment under various microwave irradiation time. PL spectra of BSA a) with and b) without urea treatment under various microwave irradiation time.

In order to demonstrate the generality of our strategy to prepare CDs, several other proteins including lipase and pepsin were applied as carbon source to prepare relevant CDs. Another denaturing agent guanidine hydrochloride (GuHCl) was also used to denature proteins. All the CDs prepared with various protein carbon sources and denaturing agents show good PL performance, and the calculated fluorescence quantum yields reach ca. 10% (Table 1). Comparatively speaking, the CDs prepared from GuHCl denatured proteins display a higher QY than that from urea denatured proteins. It has been proved that the amine molecules play dual functions as N-doping precursors and surface passivation agents for CDs as both enhanced the PL performance of CDs.[46] Compared with urea, GuHCl contributes more N-doping, which results in a better PL performance. It is mentioned that different protein carbon sources possessing various residues, and therefore we can prepare CDs covered with specific functional groups via choosing appropriate protein carbon sources as required.

Table 1. The calculated fluorescence quantum yields (QYs) of various CDs prepared with various protein carbon sources and denaturing agents.

	QY (%)
BSA+urea	13.3
BSA+GuHCl	14.4
lipase+urea	9.0
lipase+GuHCl	12.8
pepsin+urea	8.6
pepsin+GuHCl	13.1

3.3 Application performance of CDs

3.3.1 Up-conversion fluorescence behavior

Up-conversion fluorescence behavior is an attractive optical property of CDs, which enables many promising applications. Remarkably, the as-prepared CDs also show clear up-conversion fluorescence properties besides exhibiting strong luminescence in UV-to-near-infrared range. Fig. 5 shows the fluorescence spectra of CDs excited by long-wavelength light (from 680 to 820 nm) with the up-converted emissions located in the range from 440 to 460 nm. This up-converted fluorescence property of CDs should be attributed to the multi-photon active process similar to other previous reported CDs,[4] in which the simultaneous absorption of two or more photons leads to the emission of light at a shorter wavelength than the excitation wavelength (anti-Stokes type emission). These results suggest that the as-prepared CDs may also be used as a powerful energy-transfer component in photo-catalyst design for applications in environmental and energy issues. Moreover, such spectral working range overlaps spectral ranges in which water absorption vanishes, which is so-called 'first biological window' extending from 750 up to 920 nm.[47-48] Working in this spectral window does not only reduce excitation and emission-induced heating, but also minimizes light scattering in such a way that the spatial resolution of fluorescent thermal images can be improved.
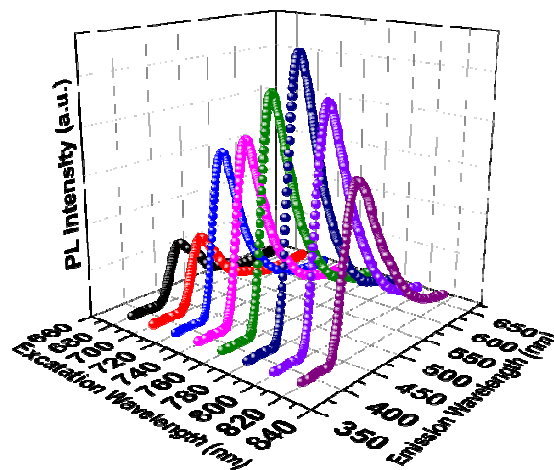
Fig. 5 Up-converted PL emission spectra of CDs.

3.3.2 CDs as pH nanosensor.

The effects of ionic strength and pH on fluorescence behavior of CDs were investigated. There is no obvious decrease in fluorescence intensity under various NaCl concentrations, indicating the good fluorescence stability of the as-prepared

RSC Advances Accepted Manuscript

CDs. The fluorescence emission of CDs were also recorded at different pH values. Interestingly, the as-prepared CDs possess a pH-sensitive fluorescence feature. As illustrated in Fig. 6, the fluorescence intensity of CDs is strong under neutral condition and weakly alkalinity (7≤pH≤9), but drops rapidly as pH decreases from 7 to 1, and remains at lower values under strong alkaline conditions (pH=11). This pH-dependent fluorescence arises from the protonation and deprotonation of carboxyl or amino groups on the surface of CDs.[49] Given such property, the CDs could be potentially used as a pH probe.
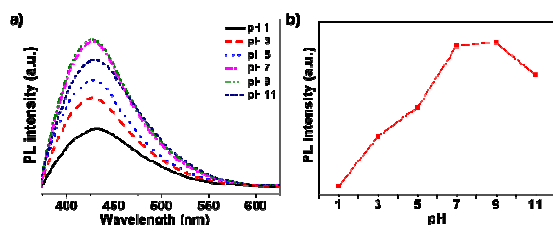
Fig. 6 a) PL spectra of CDs dispersed in solutions with different pH values (from 1 to 11); b) pH dependence of the normalized fluorescence intensity of CDs fluorescence emission.

3.3.3 CDs as thermal nanosensor.

The temperature-dependent PL behavior of the as-prepared CDs was also found. Fig. 7a records the gradual decrease of fluorescence intensity when the temperature increases from 30 to 100 ^{o}C. There is a good linear relationship with a correlation coefficient (R^2) of 0.999 between temperature and PL intensity (Fig. 7b). The temperature-response of fluorescence intensity shows an excellent reversibility during consecutive heating-cooling cycles within the temperature range of 30-100 ^{o}C (Fig. 7c). It is suggested that the temperature induced fluorescence quenching of CDs is derived from the temperature enhanced population of non-radiative channels of surface (trap/defect) states.[50-53] At low temperature, the non-radiative channels are not thermally activated; therefore, the excited electrons can radiatively emit photons. Once the temperature is increased, the non-radiative channels become thermally activated; therefore, an increasing number of the excited electrons return to the ground state through a non-radiative process, and correspondingly the fluorescence intensity decreases. This optically temperature-sensitive property provides great opportunities for design of the CDs based temperature-monitoring devices.
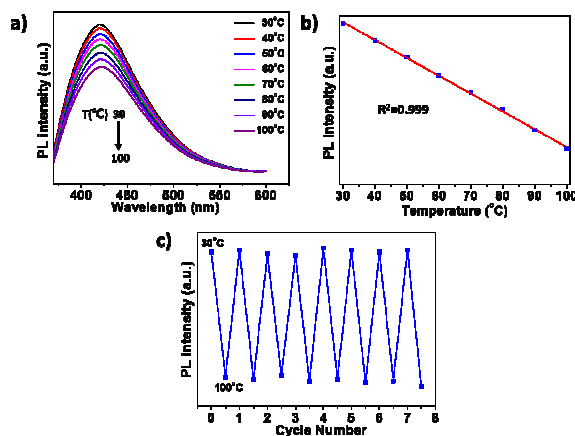
Fig. 7 a) PL spectra of CDs solution at different temperatures (30-100 ^{o}C); b) Temperature dependence of the normalized fluorescence intensity of the maximum fluorescence emission of CDs; c) The reversible temperature-dependence of fluorescence intensity over the range of 30-100 ^{o}C.

3.3.4 Sensitive and selective detection of Ag$^+$.

Considering the present of oxygen-nitrogen groups and carboxylate groups around the surface of CDs as well as the efficient fluorescent property, detection of metal ions using CDs have been reported recent years.[54-57] Therefore, in this work, we attempted to use the as-prepared CDs as a fluorescent sensing platform for different metal ions. The experimental results show that the as-prepared CDs show an extraordinary responsiveness for Ag$^+$. With the increase of the concentration of Ag$^+$ ions in the dispersion, the intensity of the fluorescent emission synchronously turns weak, indicating the quench effect of Ag$^+$ ions to the fluorescent CDs (Fig. 8a). Sensitivity of the as-prepared CDs to the Ag$^+$ ions was then carefully investigated with the concentration in the range of 0–20 μM. The relationship between the quenching ratio (I_0 - I)/I_0 and Ag$^+$ concentration is addressed in Fig. 8b, and a nice linear correlation exists over the range of Ag$^+$ concentration from 0.1 to 10 μM, giving a calibration curve of (I_0 - I)/I_0 = 0.04382×$C_{(Ag+)}$ (μM)-0.00644 with R^2 of 0.991 (inset of Fig. 8b). The limit of detection is determined to be 0.03 μM based on a signal-to-noise ratio of 3. Comparatively speaking, for the other Pb^{2+}, Mn^{2+}, Co^{2+}, Cu^{2+}, Mg^{2+}, Ni^{2+}, K$^+$, Ca^{2+}, Hg^{2+}, Al^{3+}, Fe^{3+}, NH$_4^+$, Cd^{2+}, Ca^{2+}, Mn^{2+}, Zn^{2+}, Cd^{2+} ions, there is no tremendous decrease in fluorescent intensity by adding other metal ions (10 μM) into the dispersion (Fig. 8c). These observations indicate that the fluorescent emission of CDs prepared from BSA carbon source is not only sensitive to Ag$^+$ ions but also selective to detect the Ag$^+$ ions.
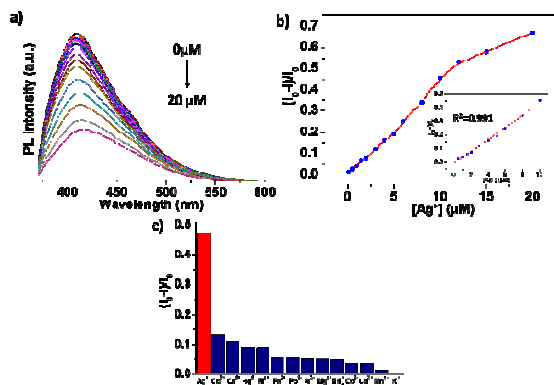
Fig. 8 a) PL spectra of CDs solution upon addition of various concentrations of Ag^+ in a pH 7.0 solution (from up to down: 0, 0.1, 0.5, 1, 1.5, 2, 3, 4, 5, 6, 8, 10, 12, 15 and 20 µM); b) The relationship between $(I_0 - I)/I_0$ and concentration of Ag^+ from 0 to 20 µM. Inset in (b) a linear region as the concentration of Ag^+ ranges from 0.1 to 20 µM. (c) Selective detection towards Ag^+ using CDs. The ions concentration is 10 µM.

Interestingly, the ions detection ability of CDs changed with the species of the chosen protein carbon source. The CDs prepared from pepsin carbon source show a specific selective detection for Cu^{2+} (Fig. 9a), while the CDs prepared from lipase carbon source show a selective detection for Ni^{2+} (Fig. 9b). This ions detection behaviour of CDs can be attributed to the corresponding ions which can quench the fluorescence of CDs presumably via electron or energy transfer.[58-59] However, the relationship between protein carbon source and ions selectivity need a further in-depth study, which might be related to certain particular amino acid residues distributed around CDs from various protein carbon source. We also monitored the time-dependent fluorescence of BSA-CDs, pepsin-CDs and lipase-CDs with various concentrations in the presence of corresponding sensitive metal ions (Fig. S3), which is very meaningful for a real application. From these results, we can see that, the detection system can reach to an equilibrium after ca. 40 minutes without stirring when diffusion mechanism dominates. However, stirring can accelerate the equilibrium of the detection system, which is benefit for shortening the span of ion detecting.
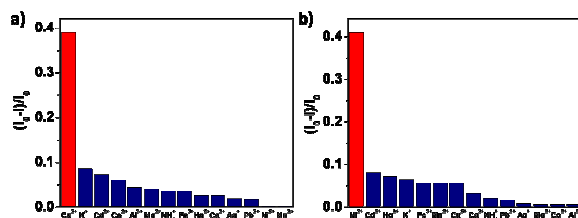
Fig. 9 a) Selective detection towards Cu^{2+} using CDs prepared from pepsin carbon source. b) Selective detection of Ni^{2+} using

CDs prepared from lipase carbon source. The concentration of ions is 10 µM.

In order to evaluate the practical utility of the present method, the CDs based fluorescent sensing platform is applied for Ag^+ assay in real water samples. The results are shown in Table 2. The Ag^+ concentration in local tap water is found to be 0. Using a standard addition method, the sample recoveries are in the range of 97-104%, and the relative standard deviations (RSDs) are between 1.5% and 2.2%, both of which are suggestive of the high accuracy and credibility of the analysis.

Table 2. Detection of Ag^+ in tap water.

Sample	Added (µM)	Found (µM)	Detected (%)	RSD (%)
1	0	0	-	-
2	1.00	0.98	98	1.8
3	3.00	3.13	104	1.5
4	5.00	5.11	102	2.2
5	7.00	6.79	97	1.6

4. Conclusions

In summary, CDs has been successfully synthesized by microwave treatment of denatured proteins. A four-step forming mechanism, including crosslinking, aromatization nucleation and growth, can be proposed. The as-prepared CDs, possessing stable visible emission and excellent up-conversion properties, exhibit a multifunctional sensing performance for pH, temperature and metal ions. Moreover, the CDs prepared from a specific protein can be sensitive to a certain metal ion. It is a very simple and devisable system for metal ions detection, which can be only accomplished by screening protein source to prepare appropriate CDs in connection with specific metal ions. The excellent sensitivity, preferable biocompatibility and nano-scale structure make the as-prepared CDs promising for intracellular imaging and temperature sensing.

Acknowledgements

Notes and references

1   S. N. Baker and G. A. Baker, *Angew. Chem. Int. Ed.*, 2010, **49**, 6726-6744.
2   H. Li, Z. Kang, Y. Liu and S. T. Lee, *J. Mater. Chem.*, 2012, **22**, 24230-24253.
3   E. J. Goh, K. S. Kim, Y. R. Kim, H. S. Jung, S. Beack, W. H. Kong, G. Scarcelli, S. H. Yun, and S. K. Hahn, *Biomacromolecules*, 2012, **13**, 2554-2561.
4   L. Cao, X. Wang, M. J. Meziani, F. Lu, H. Wang, P. G. Luo, Y. Lin, B. A. Harruff, L. M. Veca, D. Murray, S. -Y. Xie and Y. -P. Sun, *J. Am. Chem. Soc.*, 2007, **129**, 11318-11319.

5   C. Liu, P. Zhang, F. Tian, W. Li, F. Li and W. Liu, *J. Mater. Chem.*, 2011, **21**, 13163-13167.

6   W. Wang, Y. Li, L. Cheng, Z. Cao and W. Liu, *J. Mater. Chem. B*, 2014, **2**, 46-48.

7   L. Li, C. Wang, K. Liu, Y. Wang, K. Liu and Y. Lin, *Anal. Chem.*, 2015, **87**, 3404-3411.

8   B. Xu, C. Zhao, W. Wei, J. Ren, D. Miyoshi, N. Sugimoto and X. Qu, *Analyst*, 2012, **137**, 5483-5486.

9   Q. Qu, A. Zhu, X. Shao, G. Shi and Y. Tian, *Chem. Commun.*, 2012, **48**, 5473-5475.

10 Z. L. Wu, P. Zhang, M. X. Gao, C. F. Liu, W. Wang, F. Leng and C. Z. Huang, *J. Mater. Chem. B*, 2013, **1**, 2868-2873.

11 S. Sahu, B. Behera, T. K. Maiti and S. Mohapatra, *Chem. Commun.*, 2012, **48**, 8835-8837.

12 B. De and N. Karak, *RSC Adv.*, 2013, **3**, 8286-8290.

13 L. N. Wu, X. Cai, K. Nelson, W. X. Xing, J. Xia, R. Y. Zhang, A. J. Stacy, M. Luderer, G. M. Lanza, L. V. Wang, B. Z. Shen and D. P. J. Pan, *Nano Res.*, 2013, **6**, 312-325.

14 S. Y. Park, H. U. Lee, E. S. Park, S. C. Lee, J. W. Lee, S. W. Jeong, C. H. Kim, Y. C. Lee, Y. S. Huh and J. Lee, *ACS Appl. Mater. Interfaces*, 2014, **6**, 3365-3370.

15 C. J. Liu, P. Zhang, F. Tian, W. C. Li, F. Li and W. G. Liu, *J. Mater. Chem.*, 2011, **21**, 13163-13167.

16 X. H. Wang, K. G. Qu, B. L. Xu, J. S. Ren and X. G. Qu, *J. Mater. Chem.*, 2011, **21**, 2445-2450.

17 L. M. Gilbertson, J. B. Zimmerman, D. L. Plata, J. E. Hutchison and P. T. Anastas, *Chem. Soc. Rev.*, 2015, **44**, 5758-5777.

18 H. He, J. Klinowski, M. Forster and A. Lerf, *Chem. Phys. Lett.*, 1998, **287**, 53-56.

19 S. J. Zhu, Q. N. Meng, L. Wang, J. H. Zhang, Y. B. Song, H. Jin, K. Zhang, H. C. Sun, H. Y. Wang and B. Yang, *Angew. Chem. Int. Ed.*, 2013, **52**, 3953-3957.

20 P. C. Hsu and H. T. Chang, *Chem. Commun.*, 2012, **48**, 3984-3986.

21 X. F. Jia, J. Li and E. K. Wang, *Nanoscale*, 2012, **4**, 5572-5575.

22 Y. Hu, J. Yang, J. Tiana and J. S. Yu, *J. Mater. Chem. B*, 2015, **3**, 5608-5614.

23 C. Liu, P. Zhang, X. Zhai, F. Tian, W. Li, J. Yang, Y. Liu, H. Wang, W. Wang and W. Liu, *Biomaterials*, 2012, **33**, 3604-3613.

24 H. Zhu, X. Wang, Y. Li, Z. Wang, F. Yanga and X. Yang, *Chem. Commun.*, 2009, **34**, 5118-5120.

25 C. Ó' Fágáin, *Enzyme Microb. Technol.*, 2003, **33**, 137-149.

26 F. C. Meldrum, V. J. Wade, D. L. Nimmo, B. R. Heywood and S. Mann, *Nature*, 1991, **349**, 684-687.

27 M. B. Dickerson, K. H. Sandhage and R. R. Naik, *Chem. Rev.*, 2008, **108**, 4935-4978.

28 J. P. Xie, Y. G. Zheng and J. Y. Ying, *J. Am. Chem. Soc.*, 2009, **131**, 888-889.

29 J. P. Xie, Y. G. Zheng and J. Y. Ying, *Chem. Commun.*, 2010, **46**, 961-963.

30 N. Ma, A. F. Marshall and J. H. Rao, *J. Am. Chem. Soc.*, 2010, **132**, 6884-6885.

31 Y. Z. Wu, S. Chakrabortty, R. A. Gropeanu, J. Wilhelmi, Y. Xu, K. S. Er, S. L. Kuan, K. Koynov, Y. Chan and T. Weil, *J. Am. Chem. Soc.*, 2010, **132**, 5012-5014.

32 H. Wei, Z. D. Wang, L. M. Yang, S. L. Tian, C. J. Hou and Y. Lu, **Analyst**, 2010, **135**, 1406-1410.

33 C. Guo and J. Irudayaraj, *Anal. Chem.*, 2011, **83**, 2883-2889.

34 Q. Wang, X. Huang, Y. Long, X. Wang, H. Zhang, R. Zhu, L. Liang, P. Teng and H. Zheng, *Carbon*, 2013, **59**, 192-199.

35 A. T. R. Williams, S. A. Winfield and J. N. Miller, *Analyst*, 1983, **108**, 1067-1071.

36 Z. Luo, Y. Lu, L. A. Somers and A. T. C. Johnson, *J. Am. Chem. Soc.*, 2009, **131**, 898–899.

37 Z. -C. Yang, M. Wang, A. M. Yong, S. Y. Wong, X. -H. Zhang, H. Tan, A. Y. Chang, X. Li and J. Wang, *Chem. Commun.*, 2011, **47**, 11615-11617.

38 J. Wang, C. -F. Wang, and S. Chen, *Angew. Chem. Int. Ed.*, 2012, **51**, 9297-9301.

39 S. Liu, J. Q. Tian, L. Wang, H. L. Li, Y. W. Zhang and X. P. Sun, *Macromolecules*, 2010, **43**, 10078-10083.

40 S. Sahu, B. Behera, T. K. Maiti and S. Mohapatra, *Chem. Commun.*, 2012, **48**, 8835-8837.

41 J. Briscoe, A. Marinovic, M. Sevilla, S. Dunn and M. Titirici, *Angew. Chem. Int. Ed.*, 2015, **54**, 4463-4468.

42 H. Ding, S. -B. Yu, J. -S. Wei and H. -M. Xiong, 10.1021/acsnano.5b05406.

43 M. Sevilla and A. B. Fuertes, *Carbon*, 2009, **47**, 2281-2289.

44 B. J. Bennion and V. Daggett, Proc. *Natl. Acad. Sci.*, 2003, **100**, 5142-5147.

45 X. Liu, Y. Liu, Z. Zhang, F. Huang, Q. Tao, R. Ma, Y, An and L. Shi, *Chem. Eur. J.*, 2013, **19**, 7437-7442.

46 R. R. Anderson and J. A. Parrish, *J. Invest. Dermatol.*, 1981, **77**, 13-19.

47 X. Zhai, P. Zhang, C. Liu, T. Bai, W. Li, L. Dai and W. Liu, *Chem. Commun.*, 2012, **48**, 7955-7957.

48 J. V. Frangioni, *Curr. Opin. Chem. Biol.*, 2003, **7**, 626-634.

49 C. Galande, A. D. Mohite, A. V. Naumov, W. Gao, L. Ci, A. Ajayan, H. Gao, A. Srivastava, R. B. Weisman and P. M. Ajayan, *Sci. Rep.*, 2011, **1**, 85-89.

50 P. C. Chen, Y. N. Chen, P. C. Hsu, C. C. Shih and H. T. Chang, *Chem. Commun.*, 2013, **49**, 1639-1641.

51 Z. X. Gan, X. L. Wu, G. X. Zhou, J. C. Shen and P. K. Chu, *Adv. Opt. Mater.*, 2013, **1**, 554-558.

52 P. Yu, X. M. Wen, Y. R. Toh and J. Tang, *J. Phys. Chem. C,* 2012, **116**, 25552-25557.

53 Y. Hu, J. Yang, L. Jia and J. -S. Yu, *Carbon*, 2015, **93**, 999-1007.

54 L. Zhou, Y. H. Lin, Z. Z. Huang, J. S. Ren and X. G. Qu, *Chem. Commun.*, 2012, **48**, 1147-1149.

55 Q. Qu, A. W. Zhu, X. L. Shao, G. Y. Shi and Y. Tian, *Chem. Commun.*, 2012, **48**, 5473-5475.

56 W. B. Lu, X. Y. Qin, S. Liu, G. H. Chang, Y.W. Zhang and Y. L. Luo, *Anal. Chem.*, 2012, **84**, 5351-5357.

57 K. G. Qu, J. S. Wang, J. S. Ren and X. G. Qu, *Chem. Eur. J.*, 2013, **19**, 7243-7249.

58 Y. H. Chan, Y. H. Jin, C. F. Wu and D. T. Chiu, *Chem. Commun.*, 2011, **47**, 2820-2822.

59 S. Liu, J. Tian, L. Wang, Y. Zhang, X. Qin, Y. Luo, A. M. Asiri, A. O. Al-Youbi and X. Sun, *Adv. Mater.*, 2012, **24**, 2037-2041.
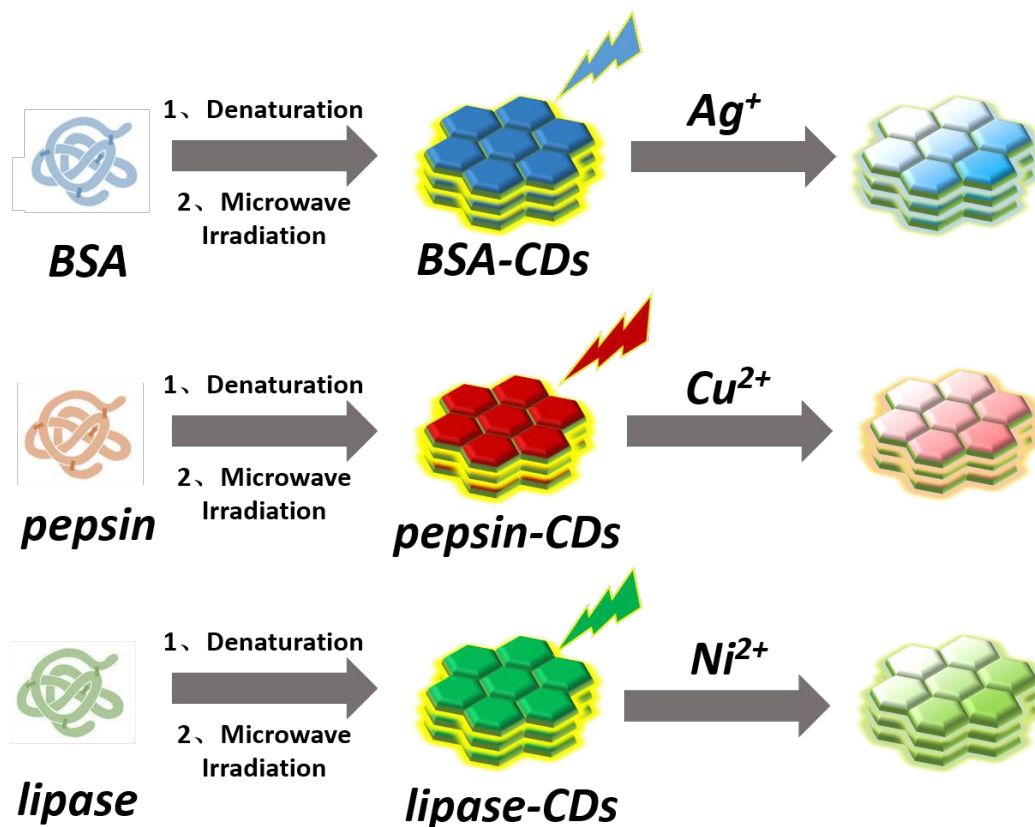
Highly photoluminescent carbon dots can be prepared through a one-step microwave treatment of the denatured proteins. The carbon dots show responsiveness for pH, temperature and metal ions. Metal ions specific detection can be realized through screening appropriate protein carbon source.